Appendices to 'From Corridor to Network Macroscopic Fundamental Diagrams: A Semi-analytical Approximation Approach'

Gabriel Tilg[1], Lukas Ambühl[2], Sérgio F. A. Batista[3], Mónica Menéndez[3], Ludovic Leclercq[4], and Fritz Busch[1]

[1]Chair of Traffic Engineering and Control, Department of Civil, Geo and Environmental Engineering, Technical University of Munich, Germany
[2]Traffic Engineering Group, Institute for Transport Planning and Systems, ETH Zurich, Switzerland
[3]Division of Engineering, New York University Abu Dhabi, United Arab Emirates
[4]Univ. Gustave Eiffel, ENTPE, LICIT, F-69518, Lyon, France

1 Nomenclature.

Table 1 summarizes the nomenclature used in this paper. They are categorized into Greek letters, as well as lower-case and capital Latin letters.

Table 1: Nomenclature

Variable	Unit	Description
$\alpha \in A$	[-]	Turning ratio in set of turning ratios
$\tilde{\alpha}$	[-]	Factor impacting the queue growth due to turning flows
β	[-]	Time-dependent capacity constraint representing traffic signals
Δt	[h]	Numerical step length in the temporal dimension
Δx	[km]	Numerical step length in the spatial dimension
ΔN	[veh]	Cycle-based difference in supply and demand
δN	[veh]	Cycle-based difference in supply and demand at a signal phase change
κ	[veh/km]	Density
κ_{max}	[veh/km]	Jam density

Table 1: Nomenclature (continued)

κ_{opt}	[veh/km]	Optimal density
κ'	[veh/km]	Transformed density
θ	[-]	Ratio of the free-flow speed u and the backward wave speed w
τ	[s]	Time between beginning of active phase and t_e
σ	[h]	Duration of spillback impact
λ	[-]	Inflow factor at origin links
γ	[-]	Factor for approximating congestion propagation
c	[s]	Cycle length
c_f	[-]	Cycle when the final vehicle reaches the intersection
g	[s]	Duration of a green phase
i, j	[-]	Indices for corridors
k	[-]	Index for intersections and links
l	[km]	Link length
m	[-]	Index for moving observer
o	[s]	Offset
p	[-]	Valid path
q	[veh/h]	Flow
q_f	[veh/h]	Flow during the cycle c_f
q_{max}	[veh/h]	Link capacity
$\tilde{q}$	[veh/h]	Maximum average flow during green phase
$\tilde{q}_d$	[veh/h]	Flow $\tilde{q}$ constrained by demand only
$\tilde{q}_s$	[veh/h]	Flow $\tilde{q}$ constrained by supply only
$\tilde{q}_{k,s}^{j \to i}$	[veh/h]	Flow $\tilde{q}$ on C^i constrained by spillbacks from C^j
r	[s]	Duration of a red phase
t	[h]	Temporal dimension
t_b	[h]	Beginning of spillback impact
t_e	[h]	End of spillback impact
t_f	[h]	Time instant when the final vehicle leaves the intersection.
$t_{k,dq}$	[h]	Time instant when the queue starts to grow at the downstream end of the link k
$t_{k,uq}$	[h]	Time instant when the queue reaches the upstream end of the link k
u	[km/h]	Free-flow speed
v	[km/h]	Speed
w	[km/h]	Backward wave speed
x	[km]	Spatial dimension
z_p	[veh]	Cost of path p
B	[-]	Curve in time and space along which the boundary data N_B is given
$C \in \mathcal{C}$	[-]	Corridor in set of corridors

Table 1: Nomenclature (continued)

$\mathcal{G}$	[-]	Hypernetwork
$I \in \mathcal{I}$	[-]	Intersection in set of intersections
K	[veh/km]	Network-wide average density
K_k	[veh/km]	Maximum density on the link k.
K_{max}	[veh/km]	Network-wide jam density
$L \in \mathcal{L}$	[-]	Link in set of links
N	[veh]	Cumulative count
N_c	[veh]	Maximum number of vehicles passing an intersection during a cycle
N_e	[veh]	Cumulative count at the end of a green phase
N_s	[veh]	Cumulative count at the start of a green phase
$\mathcal{N}$	[-]	Physical road network
$P(x,t)$	[-]	Generic point in time and space
$\mathcal{P}$	[-]	Set of valid paths from B to P
Q	[veh/h]	Network-wide average flow
$R(v_m)$	[veh]	Average maximum passing flow for a moving observer m
Z_m	[veh]	Sum of all costs along the path of a moving observer m

2 Review of the variational theory and the method of cuts

This section briefly describes the basics of VT and MC as our framework builds upon these methods. Moreover, we highlight the deficiencies of current MC-based approaches to estimate the realized network MFD.

2.1 Variational theory

Daganzo (2005a,b) formulated the VT framework to solve complex and heterogeneous KWT problems. This framework determines the cumulative number of vehicles $N(x,t)$ that have passed the location x of a road by time t, for given boundary conditions. It requires the definition of fundamental diagram(s) (FD), i.e., $q(\kappa)$, network topology including signal control settings, bottlenecks (moving or stationary), as well as boundary data N_B along a curve B. The density is denoted by κ. Recall that the FD is characterized by the free-flow speed u, the backward wave speed w, and the link jam density κ_{max}. The capacity q_{max} is derived at the optimal density κ_{opt}, i.e., $q_{max} = q(\kappa_{opt})$.

To determine the cumulative count N at a point $P(x,t)$, we need to find the valid path $p \in \mathcal{P}$ starting at the boundary B, ending at P, and leading to the minimal increase of N over p. A path p is denoted as valid if its slope lies between the extremal speeds $v \in [w,u]$ where w has a negative value. Based on

the slope of the path, costs z_p are defined. These costs refer to the maximum number of vehicles that can pass a moving observer traveling along the path p. Given the set of paths $\mathcal{P}$, as well as the associated costs z_p and boundary values $N_{B,p}$ associated with each path p, the cumulative count N_P can be found by a shortest path search as follows:

$$N_P = \min_{p \in \mathcal{P}} \{N_{B,p} + z_p\}. \tag{1}$$

By defining a numerical grid representing the solution space, we can find the cumulative count N based on eq.(1). Several possibilities for building problem-specific numerical grids exist (Daganzo and Menendez 2005). One option for signalized corridors is to define the temporal and spatial distances as Δt and Δx, respectively. Then, the points on this grid are connected with horizontal and slanted edges which slopes correspond to $v \in \{w, 0, u\}$. The cumulative number $N(x,t)$ where (x,t) are points on the numerical grid, can then be found as follows:

$$\begin{aligned} N(x,t) = \min(&N(x - \Delta x, t - \Delta t), \\ &N(x + \Delta x, t - \theta \Delta t) + \Delta x \kappa_{max}, \\ &N(x, t - \Delta t) + \beta). \end{aligned} \tag{2}$$

where $\theta = |\frac{u}{w}|$ is the absolute value of the ratio of the free-flow and the backward wave speed. If θ is an integer, the equation represents a lopsided numerical grid which facilitates the application of eq.(2), as nodes in the graph align horizontally. In cases where θ is not an integer, a shear transformation (e.g., Laval and Chilukuri 2016) can be applied to transform a triangular FD such that θ becomes an integer. Otherwise, although possible, the construction of the network becomes more cumbersome. The parameter β accounts for any capacity constraints such as traffic signals. More specifically, if $\beta = 0$ the capacity equals zero, which can for example, represent the red phase of a traffic signal. Green phases can be modelled by setting $\beta = q_{max}$. For more details, please refer to Daganzo and Menendez (2005), Leclercq and Paipuri (2019), Tilg et al. (2021).

2.2 Original method of cuts

Based on the concept of VT, Daganzo and Geroliminis (2008) introduced the MC to analytically approximate the idealized MFD for regular corridors with uniform link FD, block lengths, and signal control characteristics across all intersections. Leclercq and Geroliminis (2013) further extended the methodology to consider heterogeneous topologies, i.e., corridors with varying block lengths and signal settings. Laval and Castrillón (2015) integrated the MC into a stochastic context to be able to apply it to long corridors with varying parameters. Daganzo and Lehe (2016) formulated a linear program based on the MC to further simplify the estimation of the idealized MFD for corridors. Dakic et al. (2020) proposed a stochastic shortest path algorithm to model bi-modal interactions and their stochasticity along the corridor. A fundamental assumption of the

MC and its extensions is the existence of stationary traffic states driven by a constant inflow. In the following, we provide a brief summary of the current state of the art, and how to apply the MC for a simple example. We refer interested readers to the original papers for further details. Note that these methods estimate the idealized MFD.

MC's required parameters are the number of links in the corridor, the number of lanes, the length of each link, the signal parameters, and the FD. Similar to VT, a numerical grid is defined based on these parameters, i.e., the so-called global variational graph or *hyperlink*. However, the graph is not discretized with Δt and Δx, but consists of horizontal edges only at the location of intersections I_k referring to both green and red phases, g and r. The index k describes a link and its downstream intersection along a specific corridor. The horizontal edges are connected with slanted edges, which slopes are either equal to the free-flow speed u, or the backward wave speed w. The slanted edges start at the bottleneck termini and end where they reach the next horizontal edge representing a red phase. As in VT, costs are associated with each edge and relate to the maximum number of vehicles that would pass a moving observer traveling along such an edge. Figure 1a shows an example for a hyperlink corresponding to a corridor with two intersections I_k and I_{k+1}. The horizontal edges are defined by green and red phases g_k, g_{k+1}, r_k, and r_{k+1}.

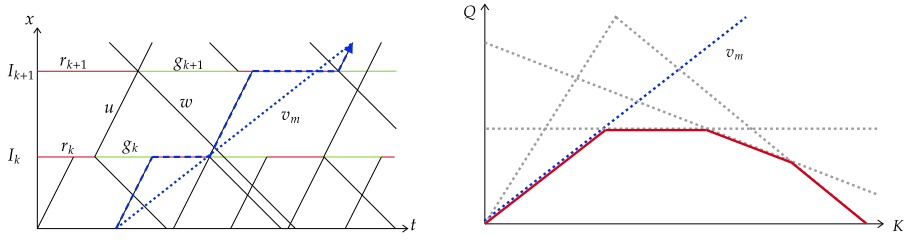

a) Example of the variational graph including the path of observer m.

b) Idealized MFD defined by a family of cuts, including the one corresponding to observer m.

Figure 1: Variational graph including a moving observer's path and its translation to the idealized MFD.

Based on the hyperlink, the idealized MFD for the given corridor can be estimated as follows. The flow q_P at a certain point $P(x, t_0)$ approaches a location-independent limit for the case of a steady state given a certain initial density. Daganzo and Geroliminis (2008) described this flow as $q = N_P/t, t = t_0 \to \infty$. The upper bound for the flow in the corridor can be derived as follows:

$$Q(K) = \inf_{v_m} \{K v_m + R(v_m)\}, \tag{3}$$

where $Q(K)$ is the average flow, K is the average density in the corridor, and v_m

is the average speed of a moving observer m. $R(v_m) = Z_m/t, t = t_0 \to \infty$ is the maximum flow that passes, on average, the moving observer m. The parameter Z_m is the sum of all costs along the path of moving observer m. This equation corresponds to a straight curve in the (Q, K) - plane and is referred to as a *cut*.

Figure 1 illustrates the procedure for a single cut as an example. The blue dashed line corresponds to the path of moving observer m. The costs Z_m are zero since only edges representing red phases and slanted edges with $v = u$ are part of the moving observer's route. The corresponding costs z of these edges are zero, as no vehicles can pass the moving observer traveling along them. The average speed v_m is displayed as a dotted blue curve. In Figure 1b the corresponding cut is shown as a blue dotted line again. Repeating this procedure, and thus evaluating eq.(3) for different K and moving observers with different average speeds v_m leads to a family of cuts, shown as the grey dotted lines in Figure 1b. These cuts constrain the average flow Q along with the evaluated range of K. The lower envelope of all cuts is the idealized corridor MFD, $Q(K)$.

3 Discussion of assumptions and limitations

- **Multimodality**: The focus lies on unimodal networks. That is, we do not consider any modes apart from private vehicles. Nevertheless, there are multimodal extensions for the original MC which can potentially be integrated into our framework. They follow the idea of representing the effects of other modes on traffic states as moving or stationary bottlenecks. We consider this, however, out of scope and leave it for future work.

- **Existence of stationary traffic states**: We assume that stationary states exist for any spatial demand pattern if the temporal change is slow. Note that this is an assumption inherited from the original MC and further applies to the general notion of the MFD (Daganzo 2007). Furthermore, we assume that such stationary states can be reached. For a given spatial demand pattern, which is represented by turning ratios at intersections in our framework, we conjecture that stationary states exist for any such pattern if the temporal demand profile is constant. Both traffic states and shock waves travel with finite speeds within a network with finite length. Thus, shock waves reach the boundaries of the network within finite time. Once all shock waves arrive at the boundary, a stationary state is reached at the network level. However, we do not explicitly specify an initial state in the network. Instead, we solve for boundary conditions which result in a maximum network-wide average flow. Thus, we implicitly assume the existence of an initial state which leads to the capacity state of the network. Note that the existence of stationary states is a common assumption in related literature (e.g., Leblanc 1975).

- **Uniqueness of stationary traffic states:** The uniqueness of stationary traffic states might not necessarily be given. On the contrary, the

results from theoretical studies for simple network topologies (e.g., two-ring networks) indicate that congested traffic states might not be unique even when being stationary, but rather depend on the initial distribution of vehicles (Jin, Gan, and Gayah 2013). However, note that we only consider two different initial states to derive the MFD. The first regards an empty network, and the second to the network at capacity. Thus, the initial states are constant. This and the fact that our node models are deterministic indicate that the resulting MFDs from our framework are unique. Nevertheless, such considerations are only valid for a slow-varying demand profile. More specifically, if the demand changes faster than the system's response can be (e.g., due to a larger network), then no stationary states will occur (e.g., Leclercq and Paipuri 2019). Daganzo (2007) introduced the system's relaxation time and further suggested approximating it by the travel time across the related region. He further stated that a change in demand should occur slowly compared to the system's relaxation time.

- **Conflicting streams**: We only consider signalized intersections without modeling conflicting streams explicitly. However, conflicting traffic streams can be approximated by reducing the average capacity of corresponding intersection approaches accordingly, e.g., based on headway distributions (Herz, Schlichter, and Siegener 1976). Related to that, other intersection types such as 4-way stops can be included if capacity estimates for the corresponding intersection approaches exist.

- **Queueing discipline**: We assume that vehicles follow a FIFO discipline on all links and at diverges (Newell 1993). Turning lanes can be introduced by splitting a link, and defining the turning ratios at the downstream end of each lane accordingly. For example, the turning ratio at the downstream end of a right-turning lane would be 1, while it would be 0 at the downstream end of the straight-going lane.

- **Intersection connectivity**: For the sake of simplicity, our framework only applies to cases where vehicles at intersections can either remain on the main corridor or change to a single adjacent corridor. Thus, only either left, right, or u-turns, but not multiple turning options can be modeled for a given link. The possibility of describing turning flows between more than a pair of corridors is left for future work. While the general framework is able to account for multiple turning options since the basic functionality requires no substantial modification, it would at least necessitate the specification of turning ratios for each option and the coupling of more than two corridors at intersections.

- **Turning ratios**: While we allow turning ratios to vary between intersections, we assume them to be constant across time. This results from our focus on deriving stationary states which cannot reasonably be achieved with time-dependent demand profiles.

- **Network-wide jam density**: When we restrict capacities at destination links, the density K is influenced by the remaining network outflow and inflow. The strongest outflow restriction is represented by a simultaneous closing of all destination links. If some links were not closed, vehicles could still leave the network. However, the queue growth throughout the network that results from the outflow restriction highly depends on the turning ratios at each intersection. A blocked intersection leads to zero flows at all downstream links independently of the respective queues. Thus, the link densities can be smaller than κ_{max}. The network inflow is determined by the maximum of the demand and the capacity of origin links. While the demand is independent of the outflow restriction, the capacity of origin links depends on whether queues have already reached these links. Due to traffic interdependencies in the network, queues can grow even though some destination links might not be restricted. In other words, a queue growing from one restricted destination link can finally block multiple origin links. Thus, for the case of a non-simultaneous outflow restriction, we assume that net outflows out of the system are larger than in the case of a simultaneous outflow restriction. Therefore, we conjecture that the maximum number of vehicles in the network, and thus K_{max} considering spatial demand patterns, can be achieved in the latter case.

- **Density transformation:** To approximate the congested branch, we mirror those traffic states by changing the sign of κ' for each traffic state (κ', q). Re-transforming the original as well as the newly generated traffic states based on eq.(27) in Section 5.3.2 of the paper, and considering K_{max} instead of the link jam density κ_{max} leads to a fully defined MFD including the congested branch. Hereby, the main assumption is that the symmetry still holds even though we utilize the reduced network jam density instead of the link jam density. This assumption is equivalent to assuming an increase of the average speed with which congestion spreads at the corridor level. Thus, also the average backward wave speed can be decreased (i.e., the value becomes more negative). This seems to be reasonable given the following example. Consider a corridor with three links in a network. Let us assume the most downstream link becomes fully congested, but then queues from adjacent corridors block the upstream intersections such that the second link remains empty, and the queue continues to grow on the most upstream link. Eventually, only the most downstream and most upstream links are fully congested, while the middle link remains empty. Congestion spreads with the corresponding shock wave speed on the most downstream link, skips the middle link, and then spreads on the most upstream link. The total time to reach a stationary state divided by the corridor length can be interpreted as the speed with which congestion spreads for this specific corridor. This speed is higher than for the case without any network effects. This corresponds to the implicit assumption that the average speed with which congestion spreads is increased, when

we apply the shear transformation using the network jam density K_{max}. Thus, we conjecture that assuming the symmetry to hold for K_{max} is reasonable.

4 Network decomposition

The initialization of the problem (Step 0) defines a physical road network $\mathcal{N}$ consisting of intersections $I \in \mathcal{I}$ and links $L \in \mathcal{L}$. Moreover, it includes the specification of signal control settings, i.e., red r and green times g, cycle lengths c and offsets o, as well as turning ratios $\alpha \in A$ at each intersection I. All information from $\mathcal{N}$ including topological features, turning ratios α, and control settings for $I \in \mathcal{I}$ have to be retained when the network is decomposed (Step 1). Note that the turning ratios are an exogenous input. The two main requirements for decomposing the network $\mathcal{N}$ are:

1. The set $\mathcal{C}$ includes all links $L \in \mathcal{L}$.
2. Each link L exists only once in $\mathcal{C}$, i.e., the corridors do not have any overlapping segments.

For small toy networks, we can determine the set $\mathcal{C}$ manually from $\mathcal{N}$. More general, realistic networks can be decomposed according to the actual layout of the roads. This includes arterials, avenues, and streets. Each road can be represented as a corridor C and as such be incorporated in $\mathcal{G}$. This will always satisfy both conditions mentioned above. Requirement 2 does not preclude the potential existence of circular routes in the network (see Tilg et al. (2021) for more details). Such interdependencies across links are essential to realistically model the propagation of traffic congestion. Note that the set $\mathcal{C}$ might affect the MFD to a certain extent.

5 Derivation of $\tilde{\alpha}$.

The maximum flow q_{max} can be written as $q_{max} = u\kappa_{opt}$ and $q_{max} = w(\kappa_{max} - \kappa_{opt})$. From this follows that:

$$u = w\frac{\kappa_{max} - \kappa_{opt}}{\kappa_{opt}}. \tag{4}$$

Furthermore, from the fundamental diagram as depicted in Figure 2 we can write:

$$\alpha q_{max} = (\kappa_{max} - \alpha\kappa_{opt})\tilde{\alpha}w. \tag{5}$$

Then, we can reformulate this equation to:

$$\tilde{\alpha} = \frac{\alpha q_{max}}{w(\kappa_{max} - \alpha\kappa_{opt})} \tag{6}$$

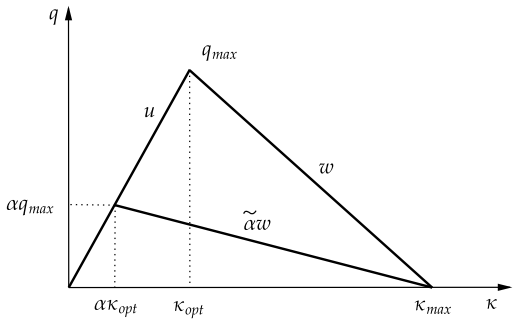

Figure 2: Illustration of $\tilde{\alpha}$ in the FD.

By putting $q_{max} = u\kappa_{opt}$, dividing by k_{opt}, and reformulating the denominator, and finally utilizing eq.(4), we get the following:

$$\begin{aligned}
\tilde{\alpha} &= \frac{\alpha q_{max}}{w(\kappa_{max} - \alpha\kappa_{opt})} \\
&= \frac{\alpha u\kappa_{opt}}{w(\kappa_{max} - \alpha\kappa_{opt})} \\
&= \frac{\alpha u}{\frac{w}{\kappa_{opt}}(\kappa_{max} - \alpha\kappa_{opt})} \\
&= \frac{\alpha u}{\frac{w}{\kappa_{opt}}(\kappa_{max} - \kappa_{opt} + (1-\alpha)\kappa_{opt})} \\
&= \frac{\alpha u}{\frac{w}{\kappa_{opt}}(\kappa_{max} - \kappa_{opt}) + \frac{w}{\kappa_{opt}}(1-\alpha)\kappa_{opt}} \\
&= \frac{\alpha u}{\frac{w}{\kappa_{opt}}(\kappa_{max} - \kappa_{opt}) + w(1-\alpha)} \\
&= \frac{\alpha u}{u + w(1-\alpha)}
\end{aligned} \tag{7}$$

This concludes the derivation of $\tilde{\alpha}$ as used in the paper.

6 Sensitivity study

6.1 Impact of route selection

An assumption made in order to reduce modeling complexity and computational burden while approximating the network MFD refers to the set of routes based on which the free-flow branch is estimated. In the nMC, we propose to estimate the free-flow branch for each corridor $C \in \mathcal{C}$ being aware that this is a simplification. In order to study the implication of this simplification, we estimate the MFD based on the nVT approach for two different sets of routes in the

network in the following. First, we evaluate the MFD based on $\mathcal{C}$, which results in 24 different routes. Second, we extract the shortest paths for all OD pairs in the Sioux Falls network and define each path as a route for which the MFD is estimated. In this case, the number of routes increases to a total of 576. Note that the capacity branch is not affected by this assumption and the congested branch equals the transformed free-flow one. Therefore, we only evaluate the free-flow branch of the MFD for the two sets of routes and compare them below.

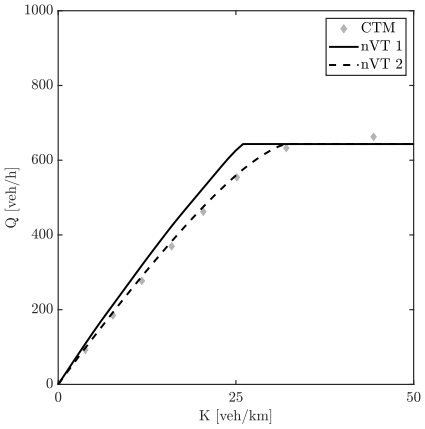

Figure 3: Comparison of the impact of route selection.

Figure 3 shows the free-flow branch of both MFDs. The solid black curve labeled as 'nVT 1' represents the derived free-flow branch based on $\mathcal{C}$. The dashed black curve 'nVT 2' illustrates the one which results from considering the second set of routes. The figure indicates that indeed the estimation's accuracy is further increased by the latter approach as the curve is closer to the ground truth MFD. However, the number of paths to be evaluated is 24 times higher in our case study. This leads to a significant increase in computational cost. In the end, the selection of routes for the MFD estimation is use-case dependent and the choice represents a trade-off between computational burden and estimation accuracy.

6.2 Impact of turning ratios

Here, we aim at evaluating our framework for the presented network with different turning ratio sets $\mathcal{A}$. More specifically, we first analyze the variability of the resulting MFDs from the ground truth to validate that spatial demand patterns indeed have an impact. Second, we compare the results from our proposed framework to the state of the art and the ground truth to assess the quality of our approach. Last, we pick a specific set $\mathcal{A}$, introduce small deviations, and investigate the effects on the resulting MFDs based on our framework. This indicates the robustness of our MFD estimation method against different spatial

demand patterns.

For the first analysis, we randomly select ten different reasonable sets $\mathcal{A}$ with turning ratios ranging again between $\alpha = [0.25, 0.75]$ with a mean at 0.5. We then evaluate the CTM ground truth, the nVT, the FS, and the LS approaches to derive the hypernetwork, and the nVT and QP approaches to approximate the network jam density K_{max}. Moreover, the state-of-the-art methods are applied. We estimate the free-flow branch only for the set $\mathcal{C}$, as we have shown in the previous section that the impact of this assumption is minor.

As the proposed methodology primarily focuses on improving the estimation of the maximum flows $\tilde{q}$ and thus the network-wide capacity Q_{max}, as well as the jam density K_{max}, we merely compare the corresponding results. This allows us to drastically reduce the scenarios to be run with the CTM. The results from the CTM simulation lead to varying Q_{max} and K_{max} for each scenario as illustrated in Figure 4. A range of about 200 veh/h for Q_{max} can be observed. The values of K_{max} cover a range of nearly 25 veh/km. The significant variability in these results shows that the MFD indeed depends on the spatial demand pattern in the network. This further indicates that a framework to estimate the MFD for specific spatial demand patterns is beneficial. Despite the assumption regarding the existence of stationary states, which might be violated in reality, the approximated MFDs can be useful.

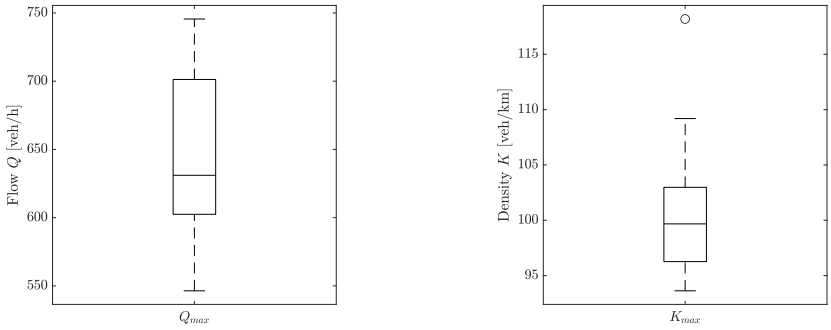

a) Q_{max} from CTM simulations with varying turning ratios.

b) K_{max} from CTM simulations with varying turning ratios.

Figure 4: Boxplots showing the variability of Q_{max} and K_{max} across the evaluated scenarios.

To further assess the nMC, we calculate the absolute relative differences ΔK_{max} and ΔQ_{max} for the MFD estimations from both the proposed framework and the state of the art, compared to the ground truth. For example, the absolute relative difference ΔQ_{max} between the nVT approach and the CTM can be calculated as $\Delta Q_{max} = |\frac{Q_{max,nVT} - Q_{max,CTM}}{Q_{max,CTM}}|$. Analogous calculations are performed to derive the other absolute relative differences. Note that Q_{max} and K_{max} for all state-of-the-art methods remain invariant across the scenarios

since they do not account for turning ratios.

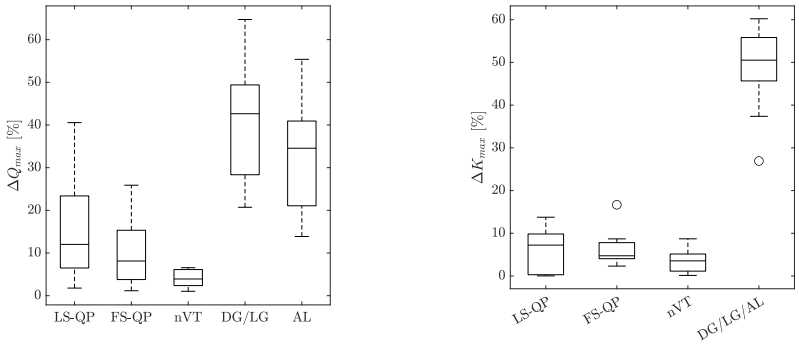

a) Absolute value of the relative difference ΔQ_{max}.

b) Absolute value of the relative difference ΔK_{max}.

Figure 5: Analysis of the estimated network-wide capacity Q_{max} and jam density K_{max}. The evaluated approaches are the proposed framework, i.e., LS-QP, FS-QP, and nVT, as well as the state of the art, i.e., DG, LC, and AL.

Figure 5 summarizes the results. Figure 5a shows the difference in the capacity estimation from the proposed LS-QP, the FS-QP, the nVT approach, and the state of the art compared to the ground truth values. The differences of the methods 'DG' and 'LG' do not vary since their estimated capacity is equal. The figure clearly shows the substantial improvement in the estimation accuracy regarding the network-wide capacity of all three proposed methods. Moreover, it is apparent that the FS-QP approach, which models network-wide spillback propagation in more detail, is more exact than the LS-QP approach, which does not account for such effects. Furthermore, the nVT approach is even more precise in estimating the network-wide capacity. The average capacity estimation of the proposed approaches is more than five times as accurate as the estimate by the state of the art. Additionally, we investigate the estimation of the network-wide maximum density K_{max} (see Figure 5b). While the average estimation of K_{max} by the nVT approach seems to be more accurate than the one by both approximate approaches, the differences are less obvious. Again, the proposed methods substantially improve the estimation of K_{max} compared to the state of the art, which assumes the jam density equal to the one of the link FD, i.e., $K_{max} = \kappa_{max}$. On average, the estimated K_{max} is more than five times closer to the ground truth value than the estimate from the state of the art.

The analysis above showed that our proposed framework has reasonable accuracy. This lets us conduct analyses that are not possible with other methods, such as the CTM, due to their high computational cost. To showcase this, we further examine the robustness of the estimated MFD with regard to small deviations of the turning ratios. To analyze the effect of small deviations of turning

ratios, we first define a reference set $\mathcal{A}$ and then introduce random variations with a maximum of $\pm 5\,\%$ relative turning flows. We sample 100 sets with different variations and evaluate the MFD for each of them based on the FS-QP approach. The results are displayed in Figure 6 as boxplots for Q_{max} and K_{max}, including the relative differences to values referring to the reference set $\mathcal{A}$. The

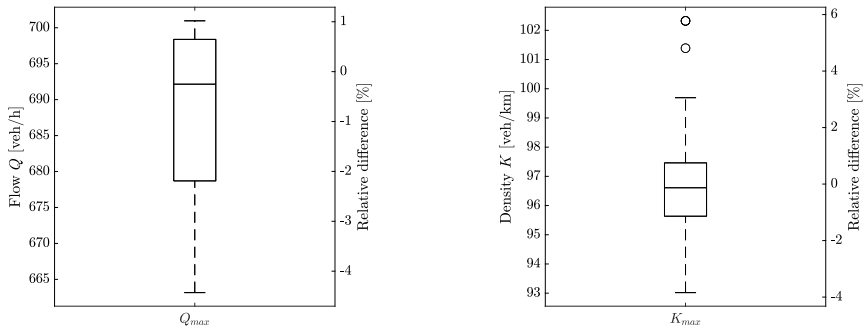

a) Q_{max} from FS-QP-based MFD estimation with varying turning ratios.

b) K_{max} from FS-QP-based MFD estimation with varying turning ratios.

Figure 6: Variability of Q_{max} and K_{max} for the evaluated scenarios with small deviations of turning ratios.

values of the capacity Q_{max} lie in a range of about 40 veh/h. Compared to the results displayed in Figure 4 which correspond to a strong variation of turning ratios, this is clearly a small range of variation. This is further highlighted by the relative differences which are below 4 %. However, it is apparent that the capacity of the estimated MFD is sensitive to turning ratios. Fortunately, due to the low computational cost of the proposed approach, one can increase the robustness of the results by simply introducing small deviations in the turning ratios and then taking the average capacity Q_{max}. Regarding the network-wide jam density, the absolute variation lies in a range of 5 veh/km. Considering that the relative differences are also below 4 %, except for two outliers, the sensitivity of the network jam density is similar to the capacity. Nevertheless, the robustness can also be increased by taking the average from an array of estimated values. These results can indicate how often the MFD has to be estimated during the day. More specifically, evaluating our proposed framework for specific turning ratios enables one to quantify how small deviations in the turning ratios affect the MFD. Thereby, one can identify the maximum variation of turning ratios for a specific intersection, or multiple ones, that corresponds to a given admissible variation of the MFD. This, in turn, allows one to identify the times of the day when the MFD has to be re-estimated to reflect variations in the turning ratios. This example further confirms that spatial demand patterns indeed impact the MFD and highlights the value the proposed framework provides for the analysis of urban traffic.

References

Daganzo CF, 2005a *A variational formulation of kinematic waves: basic theory and complex boundary conditions. Transportation Research Part B: Methodological* 39(2):187–196.

Daganzo CF, 2005b *A variational formulation of kinematic waves: Solution methods. Transportation Research Part B: Methodological* 39(10):934–950.

Daganzo CF, 2007 *Urban gridlock: Macroscopic modeling and mitigation approaches. Transportation Research Part B: Methodological* 41(1):49–62.

Daganzo CF, Geroliminis N, 2008 *An analytical approximation for the macroscopic fundamental diagram of urban traffic. Transportation Research Part B: Methodological* (42):771–781.

Daganzo CF, Lehe LJ, 2016 *Traffic flow on signalized streets. Transportation Research Part B: Methodological* 90:56–69.

Daganzo CF, Menendez M, 2005 *A variational formulation of kinematic waves: Bottleneck properties and examples. Proceedings of the 16th International Symposium on Transportation and Traffic Theory*, 345–364 (Maryland: Elsevier).

Dakic I, Ambühl L, Schümperlin O, Menendez M, 2020 *On the modeling of passenger mobility for stochastic bi-modal urban corridors. Transportation Research Part C: Emerging Technologies* 113(November 2018):146–163.

Herz R, Schlichter G, Siegener W, 1976 *Angewandte statistik für verkehrs- und regionalplaner. Verkehrs-und Regionalplaner, Werner-Ingenieur-Texte 42, Werner-Verlag, Düsseldorf* 131.

Jin WL, Gan QJ, Gayah VV, 2013 *A kinematic wave approach to traffic statics and dynamics in a double-ring network. Transportation Research Part B: Methodological* 57:114–131.

Laval JA, Castrillón F, 2015 *Stochastic approximations for the macroscopic fundamental diagram of urban networks. Transportation Research Part B: Methodological* 81:904–916.

Laval JA, Chilukuri BR, 2016 *Symmetries in the kinematic wave model and a parameter-free representation of traffic flow. Transportation Research Part B: Methodological* 89:168–177.

Leblanc LJ, 1975 *An algorithm for the discrete network design problem. Transportation Science* 9(3):183–199.

Leclercq L, Geroliminis N, 2013 *Estimating mfds in simple networks with route choice. Transportation Research Part B: Methodological* 57:468–484.

Leclercq L, Paipuri M, 2019 *Macroscopic Traffic Dynamics Under Fast-Varying Demand. Transportation Science* 53(6):1526–1545.

Newell GF, 1993 *A simplified theory of kinematic waves in highway traffic, part i: General theory, part ii: Queueing at freeway bottlenecks, part iii: Multi-destination flows. Transportation Research Part B: Methodological* 27(4):281–313.

Tilg G, Ambühl L, Batista SF, Menendez M, Busch F, 2021 *On the application of variational theory to urban networks. Transportation Research Part B: Methodological* 150:435–456.